

This paper reports the dependences that have been derived to determine the effective width of a free flange in a dangerous cross-section of the wide-flange hull girder with the breaking of the wall/edges/axis at elastic-plastic deformation depending on the applied load for a perfectly plastic material without strengthening. Currently, there are no systematic dependences to determine the effective width of the free flange of girders of this type, except for certain cases. The technique is suitable for use for both purely elastic and elastic-plastic deformation. To calculate the stressed-strained state (SSS), a finite-element method (FEM) was used to solve the three-dimensional problem from the elasticity and plasticity theory. It has been shown that the node is exposed to simple loading. The reported results were derived within the framework of the deformation theory of plasticity. The largest ratio of external load to the boundary of fluidity is 0.9. The estimation scheme takes into consideration the most unfavorable working conditions of the examined node when the safest data are acquired. The dependences were built for the theoretical coefficient of concentration in a dangerous cross-section, which is used in the proposed procedure to determine the moment of transition from the elastic stage of deformation to elastic-plastic. When determining the effective width, the complex work of the flange and its deplanation was taken into consideration by defining the SSS components in the median plane. The feasibility of the idea of designing the SSS components on the inclined plane of a free flange has been proven. In this case, there is practically a (quasi) flat stressed state, suitable for the application of classical methods to determine the effective width. The proposed technique simplifies the calculations of the strength of the examined girder

**Keywords:** elastic-plastic effective width, girder with an axis/edge/wall breaking, I-girder, concentration factor

UDC 629.5:624.04  
DOI: 10.15587/1729-4061.2021.225106

# DETERMINING THE ELASTIC-PLASTIC EFFECTIVE WIDTH OF THE FREE FLANGE OF A HULL GIRDER WITH THE BREAKING OF A WALL

V. Sokov  
Assistant\*

E-mail: valera.sokov@gmail.com

L. Korostylov

Doctor of Technical Sciences, Professor\*

E-mail: leontyy.korostilyov@nuos.edu.ua

\*Department of Structural Mechanics and Ship Construction

Admiral Makarov National University of Shipbuilding

Heroiv Ukrainy ave., 9, Mykolaiv, Ukraine, 54025

Received date 26.11.2020  
Accepted date 12.01.2021  
Published date 22.02.2021

Copyright © 2021, V. Sokov, L. Korostylov  
This is an open access article under the CC BY license  
(<http://creativecommons.org/licenses/by/4.0>)

## 1. Introduction

The object of this study is a girder in the hull of a vessel (Fig. 1) with the breaking of the wall and free flange or with the breaking of the axis.

This girder is attached by the bottom edge to the flooring, and a loose flange is attached to the broken edge to enhance the axial moment of resistance. This leads to increased strength and stiffness when bending, provides stability when squeezing axial forces are applied, and under a flat bending shape. This girder/node is the object to study its stressed-strained state (SSS) in order to create, if possible, simple engineering procedures to design it at a relatively wide variation of geometric parameters at elastic and elastic-plastic deformation. This girder can work under conditions of both elastic and elastic-plastic deformation. In the latter case, the bearing capacity of the girder increases and it can perceive much greater external loads.

Currently, there are no systematic techniques or dependences for calculating strength in general for the examined girder (Fig. 1) in official standards and marine/annual registers, except for some cases that are narrowly targeted.

At the design stage of ship structures, it is impossible to quickly assess the strength of girders with the breaking of the axis, as well as similar structures. Therefore, it is often

necessary to employ software packages in which the SSS of such girders is examined using shell or volumetric finite elements (FE).

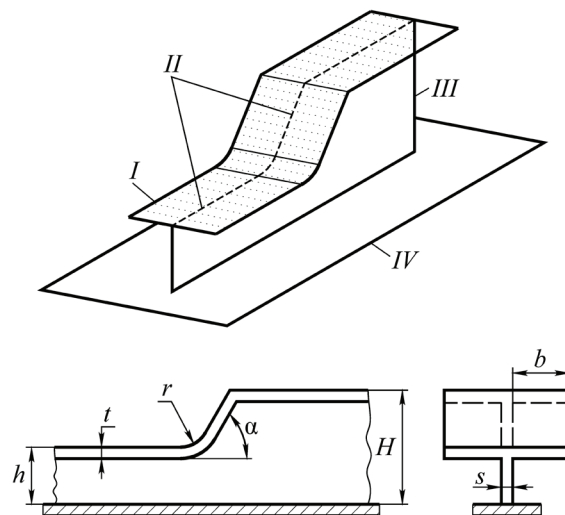


Fig. 1. General view of the examined girder with the breaking of the axis: I – free flange; II – broken edge of the wall; III – wall; IV – plating

In particular, for girders with the breaking of the wall/edges/axis, similar to the one shown in Fig. 1, there are no regular dependences to determine the effective width of the free flange, which could calculate its strength within a simple beam theory. Establishing such dependences would help save considerable time and computing resources.

---

## 2. Literature review and problem statement

---

Studies [1, 2] describe the techniques for determining the effective width of the free flange in a dangerous cross-section under elastic deformation for the girder in Fig. 1. The procedures were derived on the basis of the FEM numerical analysis. The empirical dependences of effective width yield a deviation of  $\pm 12\%$  relative to the calculated data. However, the estimation scheme adopted in the cited studies is the most conservative, which, under other milder loading conditions, could cause an increase in metal consumption; and it does not fully implement the bearing capacity of the structure.

Work [3] gives simple dependences to determine the effective width of the attached plating belt for the main links of ship structures with two-sided cladding (such as a double bottom, double board) at the boundary and elastic-plastic deformation. It is shown that under the elastic-plastic deformation, the value of effective width is greater than that under the elastic deformation, and increases with increasing load; ultimately, it equals an actual width under a boundary load. However, at the same time, the explored flanges are not free, as in a given case, but are part of the plating, which, for the case that is considered, is unacceptable.

A new method for determining the elastic-plastic effective width, based on the method of plastic lines (a kind of plasticity theory), is proposed in [4]. The method was developed for prismatic girders based on simplified assumptions, so it cannot be used for the girder on Fig. 1 in the fracture locations and on the sloping part. This relates to that a complex SSS occurs there. Also, the authors of [4] noted that currently the consideration of plasticity in determining the effective width implies adjusting elastic solutions with empirical coefficients. Although this approach produces satisfactory results but, for responsible structures, similar to the girder in Fig. 1 as part of the ship hull, may prove unacceptable.

The nonlinear shear latency by a least-square method using variable parameters of materials' characteristics is reported in [5]. However, the adopted law for the distribution of normal stresses along the transverse cross-section was obtained for prismatic girders. It is unclear if this law could be applied to the inclined part of the studied girder and in the places of flange breaking. This issue requires independent research. The authors of [5] noted the limitations of studies in general into the nonlinear shear latency and, consequently, the nonlinear (elastic-plastic) effective width.

The overview and comparison of normative documents addressing the calculation of the elastic and elastic-plastic effective width are given in [6], in order to find techniques for the studied girder in Fig. 1. Non-prismatic girders and girders with axis breaking are not discussed in [6].

Based on the results of FEM calculations, the authors of [7] derived simplified formulae to determine the effective width for the T-shaped prismatic girder. These results could hardly be applied to the prismatic sections of the studied

girder from Fig. 1 because of the effect of a plating. The examined girder refers to an I-shaped (or H-shaped) beam with asymmetrical flanges. The recommendations given in [7] cannot be used for the inclined part of the girder flange in Fig. 1 and for the places of its breaking because they were derived for a prismatic girder.

The elastic-plastic deformation of a steel girder with an H-shaped cross-section is discussed in [8], whose authors, in addition to the reported study, described a technique for determining the effective width of a flange at the elastic-plastic deformation. It is noted that in the compressed area there is a deplanation of the flange, so that this problem should be solved together with the stability problem. The shape of the H-shaped girder explored in [8] is close to the one being examined in our paper. However, in [8], both flanges are free while the lower flange of the girder in Fig. 1 is not loose; it represents part of the plating. Therefore, it is not known whether the results reported in [8] could be used for the elastic-plastic effective width regarding the free flange of the prismatic parts, not to mention the breaking places of the free flange and its inclined part.

The authors of [9] report a study of the operation of a steel regular overlap at bending by employing the FEM and empirical dependences. However, the given formulae of the elastic-plastic effective width apply to the plating that holds the prismatic longitudinal girders while the free flange of these girders was disregarded.

There are studies into the non-elastic shear latency and, correspondingly, effective width that are carried out for structures made of reinforced concrete and composite materials. These studies are also interesting because isotropic material, which is accepted for the studied girder in Fig. 1, is only a separate case of the orthotropic material involving composites.

A shear latency analysis for a composite multi-fibrous material in the elastic-plastic stage, taking into consideration the strengthening of the material, is reported in [10, 11]. However, these works consider the breakdowns/ruptures of fibrous elements, which are no longer acceptable for a conventional isotropic material of the girder shown in Fig. 1.

Based on the experimental and numerical studies, the authors of [12] derived simplified formulae for the distribution of longitudinal deformations and stresses across the width of the plate. Using them, a procedure was devised to determine the effective width depending on parameters under the effect of the boundary bending moment. The proposed distributions of longitudinal deformations are not suitable for the examined girder in places where the free flange is broken and on the sloping part where the complex SSS and deplanation occur. It is shown that under the elastic-plastic deformation the value of effective width increases compared to that at elastic deformation.

In general, our review of the scientific literature reveals that under the elastic-plastic deformation of plate elements there is an increase in the value of effective width depending on the applied load. This, in turn, leads to an increase in the bearing capacity of the structure, and, as shown in [3], the ratio of effective width to actual approaches unity when the limit loads are applied. The results reported in the available sources do not allow them to be applied to the free flange of the sloping part of the studied girder and in places of its breaking because of the existence of complex SSS there. The works we analyzed do not pay attention to the non-prismatic girders and girders with the breaking of the axis/edges/wall.

Previous studies have shown that the known thin-walled theories and shell models do not produce reliable results for the sites where a flange breaks and in adjoining areas compared to the volumetric model from the elasticity and plasticity theory.

The elastic-plastic effective width of the plating flange (called the attached belt), to which the straight edge of the examined girder is attached, can be satisfactorily determined by using, for example, works [3] or [9], as well as other earlier studies. Moreover, the dependences for calculating the elastic effective width of a given flange are well-known and are not discussed here.

Thus, the value of effective width under the elastic deformation only is the safest assessment of the effective width; however, taking into consideration it alone leads to an underestimation of the bearing capacity of the structure in general.

The problem can be stated as follows. It is required, for the girder with the breaking of the axis/edges/wall shown in Fig. 1, to devise a simple engineering and system methodology for calculating its strength in general. This is needed because, except for numerical methods such as FEM, there are no other ways to calculate girders of this type (except for single cases that are narrowly targeted).

One effective technique to assess the strength of thin-walled rods is to calculate them within the simple beam theory while taking into consideration the effective widths of flanges. Therefore, in order to solve the set problem within the framework of the proposed approach, it is necessary to derive dependences to determine the elastic-plastic effective width of the free flange with the breaking of edges; such a task has not yet been resolved.

### 3. The aim and objectives of the study

The aim of this study is to devise a procedure for calculating the effective width of the free flange under the elastic-plastic deformation in a dangerous cross-section, taking into consideration only the shear latency within the calculation of strength. This would make it possible to calculate the strength of the studied girder with the breaking of the axis by using a technical theory of beam bending. In this case, geometric characteristics should be calculated taking into consideration the effective widths of both the free flange and the plating flange (an attached belt of the plating).

To accomplish the aim, the following tasks have been set:

- to substantiate the estimation scheme and procedure for conducting research;
- to determine, for each girder variant, the minimum loads under which the plastic deformation begins;
- to determine, for each girder variant, the elastic-plastic reduction coefficient (which is the ratio of effective width to actual one) under maximum load;
- to establish, for each girder variant, the dependence of the elastic-plastic effective width of the free flange on the growing external load.

### 4. The study materials and methods

For a series of research, we developed software in the programming language C++, which employs a finite element method (FEM) to solve the volumetric problem from the theory of elasticity and plasticity.

The need to develop the software relates to the (rather tangible) difficulty in acquiring a large volume of the SSS components through existing standard subprograms and estimation packages that implement FEM. The SSS components should be determined at strictly defined places inside the body (along the lines specified by the equation) to be subsequently processed according to a certain procedure. This should be done for hundreds/thousands of the estimated node variants with different geometries.

We considered the possibility of using the following finite elements representing tetrahedrons: with the linear approximation of movements (4 nodes); with the quadratic approximation of displacements (10 nodes); with the cubic approximation of displacements (20 nodes). The finite-element procedure includes creating a grid, subsequent calculation, and processing the results. We performed numerical experiments in advance to form an optimal grid, to investigate the impact of geometric parameters on the node's SSS, to determine the boundaries of their changes. For a series of calculations, we selected finite elements with the quadratic approximation of movements, treated as the optimal choice in terms of “computation speed – minimal use of computer resources” while ensuring sufficient accuracy of the SSS results.

The object of this study is a free flange of the girder from Fig. 1 at breaking sites and on the sloping part, and the study's subject is the effective width of this flange.

## 5. Results of studying the elastic-plastic effective width of the free flange of a ship girder with the breaking of the wall

### 5.1. Substantiation of the estimation scheme and research methodology

Fig. 2 shows the symmetrical part of the estimation scheme relative to the  $xOy$  plane.

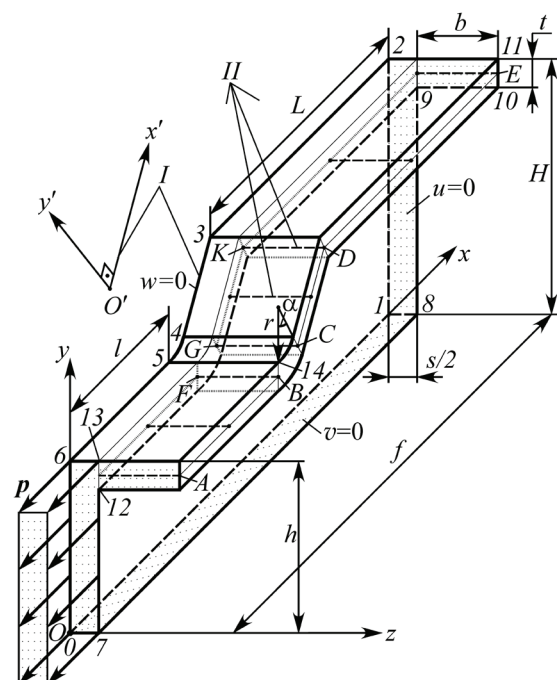


Fig. 2. Estimation scheme of the examined girder with the breaking of the wall and flange: / – parallel lines; // – the lines studied

The end of the prismatic part of a small wall in the (0–7–12–13–6) region is loaded with uniform pressure  $p$ . All points are in the plane  $y=0$ , that is, in the (0–1–8–7) region, they have no vertical movements along the  $y$  axis:  $v=0$ . All points in the end plane are  $x=f$  (where  $f$  is the distance between points 0–1), that is, in the (1–8–9–10–11–2) region, they do not have axial movements along the  $x$  axis:  $u=0$ . Given the symmetry of the structure, fasteners, and external load relative to the plane  $z=0$ , only one symmetrical part of the girder is considered, so all points in the plane  $z=0$ , that is, in the (0–1–2–3–4–5–6) region, they move  $w=0$ .

Our estimation scheme is justified by several factors. The cross-section area of the attached belt of the plating (Fig. 1) is almost always larger than the cross-section area of the free flange (taking into consideration their effective widths). Therefore, the neutral layer is always moved down to the plating and we believe that in an extreme case it coincides with the  $y=0$  layer, that is, with the (0–1–8–7) region. The examined girder during its operation mostly works on bending and stretching-compression so that the upper edges of the walls of the prismatic parts that are sufficiently distant from the breaking sites are always in the linear SSS. The described estimation scheme provides for the safest and most reliable results in comparison with other estimation schemes.

Fig. 3 shows a simplified auxiliary scheme for further explanations.

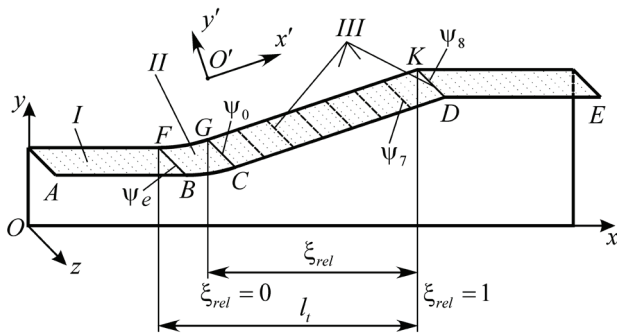


Fig. 3. Additional information: I – the median surface of the flange; II – rounding region; III – the lines studied

For further reasoning, it is necessary to explain the idea of mapping the SSS components onto the inclined plane of the flange. The SSS components were determined on the basis of this very idea. It was pointed out in [1, 2] that deforming flange blades is complex. At sites of its breaking, and in adjacent areas, there are the local bending of the plating. Studies have shown that mapping the SSS components onto the inclined part of the flange, relative to the tilted  $x'O'y'$ , made it possible to obtain an almost flat stressed state in the median plane of the flange of the inclined part of the girder. In this case, the  $x'$  axis is parallel to the flange plane, and the  $z'$  axis is parallel to  $z$ .

The normal stresses  $\sigma'_x$  relative to the  $x'O'y'$  axes, in this case, constitute the main part of the strain tensor. The distribution  $\sigma'_x$  almost coincides with the distribution of stress intensity  $\sigma_i$  along the width of the flange, even for the angle of inclination  $\alpha$  to 45–60°.

For the prismatic parts of the girder, mapping the SSS components onto the flange planes is not necessary as these planes are parallel to the  $x$  axis. The normal stresses  $\sigma_x$  relative to the  $xOy$  axes, in this case, constitute the main part of

the strain tensor. The distribution  $\sigma_x$  also almost coincides with the distribution  $\sigma_i$  across the width of the flange.

The same applies to the linear deformations  $\epsilon_x$ .

The research methodology involves the following. We collected full information on the SSS components along the studied lines (Fig. 3) that include lines  $FB$ ,  $GC$ ,  $KD$ , the sloping part lines. Then the reduction coefficients  $\psi$  were determined, representing the ratio of the effective width  $b_{ef}$  to the actual width  $b$ .

The examined lines were in the middle of the flange thickness to exclude normal stresses from the local bending of the flange plate, as shown in Fig. 2.

The effective flange width  $b_{ef}$  is determined by a formula known from [13, 14].

$$b_{ef} = \frac{1}{\sigma_{xk}} \int_0^b \sigma_x d\eta, \tag{1}$$

where  $\sigma_{xk}$  is the normal stresses in the actual flange along the line of its connection to the wall;  $\sigma_x$  is the uneven distribution of normal stresses along the width of an actual flange;  $b$  is the width of an actual flange;  $\eta$  is the coordinate in the direction perpendicular to the  $x$  axis.

The values of  $\sigma_{xk}$ ,  $\sigma_x$  should be determined by solving a flat problem from the elasticity theory for an actual belt.

As stated above, the reduction coefficient  $\psi$  is determined from the following dependence

$$\psi = \frac{b_{ef}}{b}, \tag{2}$$

where all values were explained above.

As already mentioned, the distribution of normal stresses  $\sigma_x$  (or  $\sigma'_x$ ) almost coincides with the distribution of stress intensity according to Mises  $\sigma_i$  across the width of the flange. This makes it possible to replace the value of  $\sigma_x$  (or  $\sigma'_x$ ) with  $\sigma_i$  in (1). This approach makes it possible to fully take into consideration all the SSS components. Given this, the effective width  $b_{ef}$  under the elastic-plastic deformation was determined from the following dependence

$$b_{ef} = \frac{1}{\sigma_{ik}} \int_0^b \sigma_i d\eta, \tag{3}$$

where  $\sigma_{ik}$  is the stress intensity (according to Mises) along the connection line between an actual flange and a wall;  $\sigma_i$  is the uneven distribution of stress intensity (according to Mises) across the width of an actual flange.

This study was made for an isotropic perfectly plastic material without strengthening (with a horizontal plane of fluidity). Plastic deformation was calculated within the framework of the deformation theory of plasticity because the studied node is exposed to simple loading. Our analysis of publications also reveals the predominant use of the deformation theory of plasticity (and even simpler theories that can be considered a subcategory of the deformation theory, for example [4]) in similar cases when studying the flange elastic-plastic deformation. The stressed state along the  $FB$ ,  $GC$  lines does not depend on  $H/h$  height ratios and stabilizes at  $H/h \geq 1.6$ . Therefore, the ratio of heights for all models was adopted equal to 1.6, to have a minimum volume of the node and, respectively, a minimum number of FEs. The remaining geometric parameters varied within the following limits

$$\begin{aligned}
 t/h &\in [0.02; 0.08], \quad b/h \in [0.2; 0.5], \\
 r/h &\in [0.1; 0.5], \quad \alpha \in [10^\circ; 60^\circ].
 \end{aligned}
 \tag{4}$$

It was found out that at  $l/h > 3.5$  and  $L/H > 2.5$ , even for sufficiently wide and rather thick free flanges, there is the stabilization of the SSS in the middle part of the girder. The middle part of the girder includes a sloping part with the adjacent areas of prismatic parts.

A series of calculations employed the method of elastic solutions in the iterative statement [15]. Several tests were carried out by the method of variable parameters of elasticity [16] and by the method of initial stresses in the additive/incremental statement [15, 16].

Fig. 4 shows the distribution of stress intensity  $\sigma_i$  for the selected node under the elastic-plastic deformation conditions for different types of FEs where the fluidity boundary is  $\sigma_s = 235$  MPa.

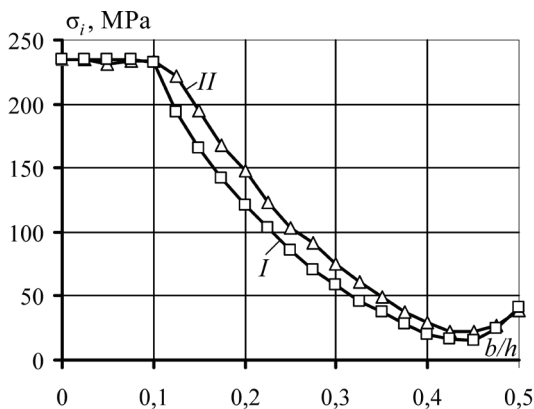


Fig. 4. Distribution of stress intensity  $\sigma_i$  along flange width under the elastic-plastic deformation conditions for a node with parameters  $r/h=0.3$ ,  $t/h=0.04$ ,  $b/h=0.5$ ,  $\alpha=30^\circ$ , under external load  $p/\sigma_s=0.9$ : I – FEs with the cubic approximation of movements; II – FEs with the quadratic approximation of movements

We calculated the studied girder under conditions of the elastic-plastic deformation for one variant as follows. We determined, for the dangerous point  $F$  at the cross-section  $FB$  (Fig. 2, 3), the concentration factor  $k_F$  under conditions of the elastic deformation only as the ratio of stress intensity (according to Mises) at point  $F$  to the value of the external load  $p$ . Next, we determined the minimum load  $p_{\min} = \sigma_s/k_F$ , (where  $\sigma_s$  is the fluidity limit), at which plastic deformation begins across the dangerous cross-section  $FB$ . The elastic-plastic work of the free flange for each variant studied was calculated for three external load values  $p_i$ , which were determined from the following formulae

$$\left. \begin{aligned}
 p_i &= \begin{cases} p_{\min} + k_{pi} \cdot \Delta p, & \text{if } p_{\min} < [\sigma] \\ p_{\min} = [\sigma], & \text{if } p_{\min} \geq [\sigma] \end{cases} \\
 i &= 1, 2, 3, \\
 k_{pi} &= 0, 3i = [0.3; 0.6; 0.9], \\
 \Delta p &= \sigma_s - p_{\min}, \\
 p_{\min} &= \frac{\sigma_s}{k_F}, \quad [\sigma] = 0.9\sigma_s.
 \end{aligned} \right\}
 \tag{5}$$

It should be noted that for some variants of the node (mainly for sloping girders), the number of load options  $p_i$  was less than three, owing to the structure of the first equation (5).

The mechanism of the girder flange plastic deformation is as follows. With the gradual growth of external load, plastic deformation begins in the cross-section/line  $FB$ , then proceeds to the  $CG$  cross-section, and then spreads to the inclined part of the flange gradually to the top with a higher wall height. Within the framework of the current study, we give dependences for reduction coefficient (2) precisely for the  $FB$  cross-section under the elastic-plastic deformation because it is dangerous in terms of the emergence of plasticity. For the adopted upper value of the external load  $p=0.9\sigma_s$  (Fig. 2), plastic deformation occurs in the region of the rounding  $FBCG$  and adjacent areas while the sloping part is mostly exposed to elastic deformation. In the end, the carrying capacity at extreme loads is assessed on the basis of a dangerous cross-section, which is the  $FB$  cross-section. The boundary analysis is not considered.

### 5. 2. Determining the minimum loads that cause the emergence of the elastic-plastic deformation of a free flange

An important parameter in the study of elastic-plastic deformation was the concentration factor  $k_F$ , owing to which it is possible to determine the loading at which the plastic deformation of the flange begins.

An empirical dependence for the concentration factor  $k_F$  on the geometric parameters of the node studied at point  $F$  (Fig. 2, 3), can be represented as follows

$$\left. \begin{aligned}
 k_F &= a_0 \tanh(a_1 \alpha); \\
 c_0 &= 30 \tanh(30 b_h^3); \quad c_1 = -50 b_h - 14; \\
 b_0 &= c_0 r_h + c_1; \quad b_1 = 6.4 r_h + 2.6 b_h + 4.7; \\
 a_1 &= b_0 t + b_1; \quad a_0 = (r_h - 0.59)(t_h - 0.28) \times \\
 &\times (b_h + 7.4) + 0.15 a_1; \\
 r_h &= r/h; \quad t_h = t/h; \quad b_h = b/h; \quad \alpha, \text{rad.}
 \end{aligned} \right\}
 \tag{6}$$

Dependence (6) determines the concentration factor  $k_F$  with a deviation of  $\pm 7\%$  relative to the data obtained from FEM. For example, for parameters  $r/h=0.3$ ,  $t/h=0.04$ ,  $b/h=0.5$ ,  $\alpha=30^\circ$ , the concentration factor value  $k_F=1.555$ .

Fig. 5 shows the selected dependences of the reduction coefficient  $\psi$  from formula (2) on the applied load for the cross-section/line  $FB$ . The bottom point of each diagram corresponds to the condition when the flange is under the elastic deformation conditions, just before the onset of plasticity, for load  $p_{\min}$  determined in (5).

The first selected group of parameters in Fig. 5,  $a$  includes the 1-4 curves with the following parameters: 1 –  $r/h=0.1$ ;  $t/h=0.04$ ;  $b/h=0.5$ ;  $\alpha=30^\circ$ ; 2 –  $r/h=0.1$ ;  $t/h=0.04$ ;  $b/h=0.2$ ;  $\alpha=30^\circ$ ; 3 –  $r/h=0.1$ ;  $t/h=0.04$ ;  $b/h=0.5$ ;  $\alpha=20^\circ$ ; 4 –  $r/h=0.5$ ;  $t/h=0.04$ ;  $b/h=0.5$ ;  $\alpha=20^\circ$ .

The second selected group of parameters in Fig. 5,  $b$  includes the 5-7 curves with the following parameters: 5 –  $r/h=0.3$ ;  $t/h=0.02$ ;  $b/h=0.5$ ;  $\alpha=20^\circ$ ; 6 –  $r/h=0.3$ ;  $t/h=0.04$ ;  $b/h=0.5$ ;  $\alpha=20^\circ$ ; 7 –  $r/h=0.3$ ;  $t/h=0.02$ ;  $b/h=0.5$ ;  $\alpha=45^\circ$ .

The first selected parameter group makes it possible to track the dependence of the reduction coefficient  $\psi$  on the relative width  $b/h$ , the relative radius  $r/h$ , and the angle of inclination  $\alpha$  at a constant flange thickness  $t$ . The second selected group of parameters makes it possible to track the

dependence of the reduction coefficient  $\psi$  on the relative thickness  $t/h$  and the angle of inclination  $\alpha$  at a constant flange width  $b$  and the rounding radius  $r$ .

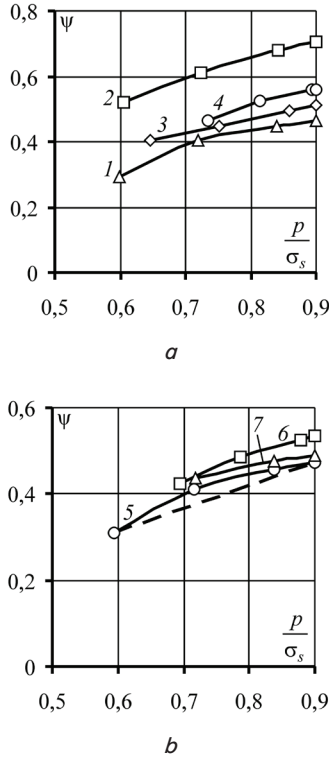


Fig. 5. The dependence of the reduction coefficient  $\psi$  on relative load under the conditions of plastic deformation:  $a$  – dependences for the first selected group of parameters;  $b$  – dependences for the second selected group of parameters

**5. 3. The elastic-plastic reduction coefficient of flange width at maximum load**

For the relative load  $p/\sigma_s=0.9$ , the value of the reduction coefficient  $\psi_{0.9}$  depending on the geometric parameters can be determined from the following empirical dependence

$$\left. \begin{aligned} \psi_{0.9} &= a_0 \exp(a_1 b_h); \\ b_0 &= 0.11 \ln r_h + 3.17 t_h + 0.87; \\ \beta &= 0.25 r_h + 0.56 t_h - 0.23; \\ a_0 &= b_0 \alpha^\beta; \\ d_0 &= 0.48 r_h - 6.10 t_h - 1.085; \\ \gamma &= (2.2 t_h - 0.2) \ln r_h + 0.28 \ln t_h + 0.77; \\ a_1 &= d_0 \alpha^\gamma; \\ b_h &= b/h; r_h = r/h; t_h = t/h; \alpha, \text{ rad.} \end{aligned} \right\} \quad (7)$$

Formula (7) determines the value of the reduction coefficient  $\psi_{0.9}$  with a relative error not exceeding  $\pm 10\%$  relative to the results obtained from FEM for the range of geometric parameters (4).

For the relative load defined within the limits  $0.78 \leq p/\sigma_s \leq 0.82$ , corresponding to  $p/\sigma_s \approx 0.8$ , the value of the reduction coefficient  $\psi_{0.8}$  depending on the geometric parameters can be determined from the following empirical dependence

$$\left. \begin{aligned} \psi_{0.8} &= a_0 \exp(a_1 b_h); \\ b_0 &= 0.11 \ln r_h + 0.78 t_h + 0.92; \\ \beta &= 0.514 r_h - 6.2 t_h - 0.088; \\ a_0 &= b_0 \alpha^\beta; \\ d_0 &= 0.27 r_h + 3.3 t_h - 1.31; \\ \gamma &= (7 t_h - 0.1) \ln r_h - 0.19 \ln t_h - 0.61; \\ a_1 &= d_0 \alpha^\gamma; \\ b_h &= b/h; r_h = r/h; t_h = t/h; \alpha, \text{ rad.} \end{aligned} \right\} \quad (8)$$

Formula (8) determines the value of the reduction coefficient  $\psi_{0.8}$  with a relative error not exceeding  $\pm 8\%$  relative to the results obtained from FEM for the range of geometric parameters (4).

Already for the relative load defined within the limits  $0.68 \leq p/\sigma_s \leq 0.72$ , corresponding to  $p/\sigma_s \approx 0.7$  only 10% of the calculated variants of the total number would undergo the elastic-plastic deformation. These are the nodes with a high concentration factor at point  $F$  (Fig. 2, 3), having a large angle of  $\alpha$ , at a low ratio of  $r/h$ .

For the relative load  $p/\sigma_s=0.9$  over 90% (93% in this case) of the total number of variants of the node adopted for a series of calculations are under the conditions of elastic-plastic deformation. For the range  $0.78 \leq p/\sigma_s \leq 0.82$ , corresponding to  $p/\sigma_s \approx 0.8$ , only a third (32% in this case) of the node variants operate in an elastic-plastic region. Formula (8) should be used as an estimate, despite its high accuracy, because it is defined for the relative load range, albeit narrow. Before using formulae (7) or (8) for the reduction coefficient  $\psi$ , make sure that the node is exposed to the elastic-plastic deformation. To this end, the following condition must be met

$$p_{\min}^{rel} \leq p^{rel}; p_{\min}^{rel} = 1/k_F; p^{rel} = p/\sigma_s, \quad (9)$$

where  $k_F$  is defined from (6);  $p_{\min}^{rel}$  is the minimal relative load at which the elastic-plastic deformation of the free flange begins in a dangerous cross-section, starting from point  $F$ ;  $p^{rel}$  is the relative load equal to 0.9 for (7) and  $\approx 0.8$  for (8).

For example, for the above parameters  $r/h=0.3$ ,  $t/h=0.04$ ,  $b/h=0.5$ ,  $\alpha=30^\circ$ , plastic deformation in a dangerous cross-section begins at the relative load  $p_{\min}^{rel} = 1/k_F = 1/1.555 = 0.64$ , which makes it possible to apply both (7) and (8) based on (9). For the relative load  $p^{rel} \approx 0.8$ , the reduction coefficient value determined from formula (8) is  $\psi_{0.8} = 0.4983$ . For  $p^{rel} = 0.9$ , the reduction coefficient value from (7) is  $\psi_{0.9} = 0.5287$ . We observe an increase in the reduction coefficient with an increase in the value of the applied load.

**5. 4. The dependence of the elastic-plastic effective width of a free flange on a growing external load**

To simplify calculations and derive a reliable assessment of the reduction coefficient and, accordingly, effective width, the curves that approximate the dependence of the reduction coefficient on relative load (Fig. 5) are replaced with straight lines. These straight lines connect the ends of the curves, as shown for line 5 in Fig. 5.

Thus, the resulting effective width is always smaller than it actually is, which is a safe assessment.

To build a linear dependence, one needs to know the coordinates of two points. The coordinate of the top point is known ( $p^{rel}=0.9$ ;  $\psi_{0.9}$  from (7)).

To determine the coordinate of the bottom point for each diagram in Fig. 5, it is necessary to have a dependence of the reduction coefficient on geometric parameters under the conditions of elastic deformation. Elastic deformation has special features, not discussed in the current paper, explaining them is beyond it. This is because under the conditions of elastic deformation each layer of a flange parallel to the median plane is in the SSS different from the state in the adjacent layers, as opposed to elastic-plastic deformation. Elastic deformation should be considered for breaking sites and a sloping part and construct regression dependences for dangerous *FB* and *GC* cross-sections and along the sloping part. Elastic-plastic deformation affects only the transition area from a low wall height to the sloping part *FBCG*; the *FB* cross-section is more dangerous. With purely elastic deformation, a more dangerous cross-section can be *CG*.

For a dangerous *FB* cross-section under conditions of the flange elastic deformation only, the reduction coefficient  $\psi_e$  can be determined from the following dependence [2]

$$\left. \begin{aligned} \psi_e &= \psi'_r - 0.05 \sin(0.45 \psi'_r), \\ \psi'_r &= a_2 b_h^{\beta}, \\ a_0 &= (2.8r_h + 0.74)t_h + 0.19r_h - 0.95, \\ a_1 &= \frac{0.24r_h + 0.42}{t_h^{0.6}}, \quad a_2 = a_0 \tanh(a_1 \alpha) + 1.023, \\ \beta &= 0.16 - (0.28r_h + 1) \exp(-(0.05 \ln(r_h) + 1.94)a_2), \\ t_h &= t/h, \quad b_h = b/h, \quad r_h = r/h, \quad \alpha, \text{ rad.} \end{aligned} \right\} \quad (10)$$

Dependence (10) determines the  $\psi_e$  coefficient with  $a \pm 12\%$  accuracy relative to the data calculated from FEM for the range of geometric parameters

$$\left. \begin{aligned} t/h &\in [0.02; 0.1], \quad b/h \in [0.1; 0.5], \\ r/h &\in [0.1; 0.5], \quad \alpha \in [3^\circ; 60^\circ], \\ H/h &\in [1.6; 2.8], \\ \text{and } H/h &< 1.6 \text{ if } l_t/h > 5.4. \end{aligned} \right\} \quad (11)$$

For the above parameters,  $r/h=0.3$ ,  $t/h=0.04$ ,  $b/h=0.5$ ,  $\alpha=30^\circ$ , the reduction coefficient at elastic deformation is  $\psi_e=0.3381$ .

Table 1 gives, in a compact form, the calculated values for the selected node parameter.

Table 1

Calculated values for the examined node with parameters  $r/h=0.3$ ,  $t/h=0.04$ ,  $b/h=0.5$ ,  $\alpha=30^\circ$

No. of entry	Concentration factor $k_F$	Minimum relative loading at which the elastic-plastic deformation begins, $p_{min}^{rel}$	Reduction coefficient at elastic deformation $\psi_e$	Reduction coefficient at elastic-plastic deformation	
				$p^{rel} \sim 0.8$ , $\psi_{0.8}$	$p^{rel} = 0.9$ , $\psi_{0.9}$
1	1.555	0.64	0.3381	0.4983	0.5287

To determine the reduction coefficient  $\psi(p^{rel})$  at elastic-plastic deformation depending on the applied load

within the proposed approach, one can use the following dependence

$$\psi(p^{rel}) = \frac{(p^{rel} - p_{min}^{rel})(\psi_{0.9} - \psi_e)}{0.9 - p_{min}^{rel}} + \psi_e, \quad (12)$$

where all the values have been explained above.

Thus, the procedure of calculating the reduction coefficient  $\psi$  and, accordingly, the effective width  $b_{ef}$  under conditions of the elastic-plastic deformation of a free flange of the studied girder in Fig. 1 in a dangerous cross-section *FB* can be represented as follows:

- 1) for the selected/predefined geometric parameters of the examined node in Fig. 1, determine the concentration factor  $k_F$  from (6);
- 2) determine the reduction coefficient at elastic deformation  $\psi_e$  from (10);
- 3) determine the relative loading  $p^{rel}$  from expression 3 in (9) for the applied external load  $p$ ;
- 4) determine the minimum relative loading  $p_{min}^{rel}$  from expression 2 in (9), at which the elastic-plastic deformation begins;
- 5) check condition 1 in (9). If condition 1 is met, the flange is in a state of elastic-plastic deformation; proceed to point 6. If condition 1 in (9) is not met, the flange is in a state of elastic deformation only; in this case, the reduction coefficient is  $\psi = \psi_e$  calculated in point 2; the effective width  $b_{ef}$  is found from (2); at this stage, one should be stopped;
- 6) calculate the reduction coefficient  $\psi_{0.9}$  from (7), which corresponds to the relative loading  $p^{rel}=0.9$  for elastic-plastic deformation;
- 7) apply formula (12) to determine the reduction coefficient  $\psi(p^{rel})$  under the conditions of elastic-plastic deformation depending on the applied relative loading  $p^{rel}$ ; apply (2) to find the effective width  $b_{ef}$ .

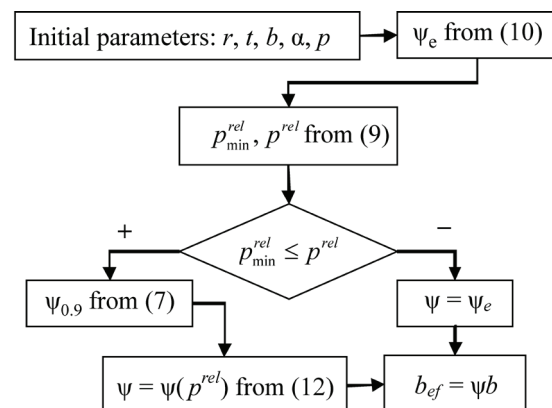


Fig. 6. Flowchart of the algorithm for determining the reduction coefficient  $\psi$  and the effective width  $b_{ef}$  at elastic-plastic deformation

The above procedure for calculating effective width under the elastic-plastic deformation is represented below in Fig. 6 in the form of an algorithm flowchart.

To take into consideration an error in the empirical formulae, the values of the reduction coefficients  $\psi_{0.9}$ , ( $\psi_{0.8}$ ),  $\psi_e$  must be multiplied by 0.9 (more precisely, by 0.892 for a 12% deviation in the worst case) for individual calculations and/or before using (12).

**6. Discussion of results of studying the elastic-plastic effective width of a free flange**

With an increase in effective width, which occurs under a growing external loading, there is an increase in the geometric characteristics of the girder, associated with the calculation of plasticity. The increase in these characteristics leads to an increase in the boundary (dangerous) moment that a girder can withstand within the framework of an elastic-plastic or boundary analysis. In this case, the actual cross-section remains unchanged. That is, we observe an increase in the resistance of the girder without changing its structure. This makes it possible to better utilize the bearing capacity of the studied girder in general, which leads to a decrease in its metal consumption without increasing manufacturability, which is very relevant for ship structures. The reported procedure makes it possible to carry out independent calculations of strength, or could be used as an addition to the objective functions as constraints for further optimal research under the conditions of elastic-plastic deformation of the studied girder.

The diagrams in Fig. 5 and dependence (12) demonstrate that with the growth of the external loading under the conditions of elastic-plastic deformation, the value of effective width only increases. This is because the area under the diagram of stress intensity  $\sigma_i$ , which matches the integral in expression (3), increases with increasing load. Accordingly, the value of the elastic-plastic effective width, determined from formula (3), increases. The growth of the area is because the region of plastic deformation of the flange along its width increases with increasing load. We explain it as follows. Fig. 4 shows the diagram  $\sigma_i$  for the specified parameters; it does not matter that for the relative loading  $p/\sigma_s=0.9$ . The plastic region corresponding to the horizontal area of the  $\sigma_i$  distribution area is from  $b/h=0$  to  $b/h \approx 0.1$ . When the external loading increases, ranging from  $p/\sigma_s=0.9$  and above, the plastic flange area increases as well while the horizontal region on the diagram becomes longer. In this case, the  $\sigma_i$  diagram becomes fuller; the area under the  $\sigma_i$  diagram is greater, accordingly; and the intensity of stresses  $\sigma_{ik}$  along the connection line between an actual flange and the wall, defined in (3), does not change. After all, if the external loading  $p/\sigma_s \rightarrow 1.0$ , the reduction coefficient  $\psi$  also approaches 1, and the effective width  $b_{ef}$  approaches an actual width  $b$ . That is, at  $p/\sigma_s \rightarrow 1.0$ , we obtain  $\psi \rightarrow 1.0$ ,  $b_{ef} \rightarrow b$ .

To explain the latter statement and further confirm the above, it is more convenient to rewrite an expression for the reduction coefficient (2) as follows

$$\psi = \frac{b_{ef}}{b} = \frac{\sigma_{imid}}{\sigma_{ik}}, \quad \sigma_{imid} = \frac{1}{b} \int_0^b \sigma_i d\eta, \tag{13}$$

where  $\sigma_{imid}$  is the average value of stress intensity  $\sigma_i$ ;  $\sigma_{ik}$  is the stress intensity (according to Mises) along the connection line between an actual flange and a wall; the remaining values were explained above for formulae (2), (3); expression (13) was derived using formulae (2), (3).

Thus, if  $p/\sigma_s \rightarrow 1.0$ , the distribution of  $\sigma_i$ , in this case, represents a horizontal line along the entire width of the flange, whose equation is  $\sigma_i = \sigma_s$ . In this case, the intensity of stresses  $\sigma_{ik}$  is equal to the average stresses  $\sigma_{imid}$  defined by expression 2 in (13), which both equal the boundaries of fluidity  $\sigma_s$ , that is,  $\sigma_{ik} = \sigma_{imid} = \sigma_s$ . As a conclusion from expression 1

in (13), the reduction coefficient is equal to unity. These explanations are confirmed by a review of the literature.

The proposed method takes into consideration all components of the SSS, due to the use of the intensity of stresses  $\sigma_i$  in (3) instead of only  $\sigma_x$  in (1), given the almost identical distributions of  $\sigma_i$  and  $\sigma_x$ . The use of stress intensity makes it possible to better track plastic deformation. In the proposed method, side effects caused by complex flange deformation at breaking sites and adjoining areas are discarded. Specifically, additional bending stresses are not taken into consideration, caused by the local bending of a flange plane, because the SSS components, in this case, are determined at the median surface of the flange. The proposed method for determining effective width, first developed for girders with the breaking of edges/axis/wall, could be used immediately for the elastic and elastic-plastic deformation.

This study is characterized by general limitations inherent in determining effective width. As one knows, the effective width depends in a general case on the conditions of fastening, the type and kind of loading, geometric parameters, material, and other factors of the plate element. Effective width is a variable value along the length of the flange. The elastic-plastic effective width additionally depends on the amount of the external loading at the same type and kind of it. There are many other factors that affect the effective width, in particular physical, technological, operational, etc. However, a given method is limited to use only for a dangerous cross-section. Moreover, determining the effective width is due to taking into consideration only shear latency in terms of strength, not including loss of stability. The type of external loading and fastening conditions take into consideration the most adverse case, which, although it leads to safe results, does not fully exhaustively actualize the bearing capacity of the girder. The studied girder should be only under the conditions of transverse bending.

In the future, it is possible to advance this method for the entire inclined part of the studied girder, as the viability of the idea of mapping the SSS components onto the inclined flange plane has been proven. Softer operational conditions and loads can be applied, which could lead to even more complete consideration of the bearing capacity of this girder. However, in this case, the designer/constructor must guarantee certain operating conditions. A very separate study is to determine the effective width of the free flange taking into consideration the loss of stability. One can take into consideration the impact of the weld, the presence of cutouts, structural reinforcements, etc. The study of girders with the breaking of the axis is accompanied by a lack of analytical solutions and intensive use of numerical methods.

**7. Conclusions**

1. The most conservative estimation scheme was developed to investigate SSS that yields the safest results. The devised research methodology makes it possible to examine each girder variant only from the moment of the emergence of plasticity. The idea of mapping the SSS components onto the inclined plane of a free flange has fully confirmed its right to exist. In this case, there is almost a flat stressed state where the distribution of stress intensity almost coincides with the distribution of normal stresses determined relative to the tilted axes. These normal stresses constitute the main

part of the strain tensor. This makes it possible to apply well-known procedures to determine the effective width and further conduct research for the inclined part of the flange.

2. The minimum relative loading at which plastic deformation begins is defined as an inverse value to the theoretical factor of concentration in a dangerous cross-section. In turn, we have built empirical dependences for the theoretical concentration factor depending on the geometric parameters of the studied node.

3. We have constructed dependences for the reduction coefficients used to calculate effective widths, depending on parameters, for the fixed values of maximum loading of 0.8 and

0.9 on the fluidity limit. In this case, the dependences of the reduction coefficient for a load of 0.9 on the fluidity limit are more accurate. Therefore, they are used in further reasoning.

4. A procedure to calculate the elastic-plastic effective width of a free flange has been devised, depending on the geometric parameters of the girder and external load for a dangerous cross-section. The technique could be used for purely elastic deformation. It is shown that the linearization of the dependences of the reduction coefficient on the applied loading always produces safe results. The procedure has been described; the formulae have been given; a flowchart of the algorithm to apply the developed method has been represented.

#### References

1. Sokov, V. M. (2020). Veryfikatsiia ta modyfikatsiia formuly V. P. Suslova dlia efektyvnoi shyryny vilnoho poiasku balky zi zlamom stinky. Suchasni tekhnolohiyi proektuvannia, pobudovy, ekspluatatsiyyi i remontu suden, morskykh tekhnichnykh zasobiv i inzhenernykh sporud: materialy vseukrainskoi naukovo-tekhnichnoi konferentsiyyi z mizhnarodnoiu uchastiu. Mykolaiv: NUK, 106–110.
2. Sokov, V. M. (2020). Efektyvna shyryna vilnoho flantsia sudnovoi balky zi zlamom stinky v nebezpechnomu pererizi. Inovatsiyyi v sudnobuduvanni ta okeanotekhnitsi: materialy XI mizhnarodnoi naukovo-tekhnichnoi konferentsiyyi. Mykolaiv: NUK, 233–236.
3. Belenkiy, L. M., Raskin, Y. N., Vuillemin, J. (2007). Effective plating in elastic–plastic range of primary support members in double-skin ship structures. *Marine Structures*, 20 (3), 115–123. doi: <https://doi.org/10.1016/j.marstruc.2007.06.002>
4. Hansen, T., Gath, J., Nielsen, M. P. (2010). An improved effective width method based on the theory of plasticity. *Advanced Steel Construction*, 6 (1), 515–547. doi: <https://doi.org/10.18057/ijasc.2010.6.1.1>
5. Lin, Z., Zhao, J. (2012). Modeling inelastic shear lag in steel box beams. *Engineering Structures*, 41, 90–97. doi: <https://doi.org/10.1016/j.engstruct.2012.03.018>
6. Yemelin, Y. (1992). On the effective width of girder flanges in elastic and elasto-plastic stages. *Journal of Constructional Steel Research*, 21 (1-3), 195–204. doi: [https://doi.org/10.1016/0143-974x\(92\)90027-c](https://doi.org/10.1016/0143-974x(92)90027-c)
7. Shi, Q.-X., Wang, B. (2015). Simplified calculation of effective flange width for shear walls with flange. *The Structural Design of Tall and Special Buildings*, 25 (12), 558–577. doi: <https://doi.org/10.1002/tal.1272>
8. Cheng, X., Chen, Y., Pan, L. (2013). Experimental study on steel beam–columns composed of slender H-sections under cyclic bending. *Journal of Constructional Steel Research*, 88, 279–288. doi: <https://doi.org/10.1016/j.jcsr.2013.05.020>
9. Erkmen, B., Kilic, B. T. (2019). Determination of Effective Breadth Width of Steel Plate Stiffener Based on Nonlinear FE Analysis. *The 14th Nordic Steel Construction Conference*, 3 (3-4), 829–834. doi: <https://doi.org/10.1002/cepa.1141>
10. Okabe, T., Takeda, N. (2002). Elastoplastic shear-lag analysis of single-fiber composites and strength prediction of unidirectional multi-fiber composites. *Composites Part A: Applied Science and Manufacturing*, 33 (10), 1327–1335. doi: [https://doi.org/10.1016/s1359-835x\(02\)00170-7](https://doi.org/10.1016/s1359-835x(02)00170-7)
11. Kimura, S., Koyanagi, J., Hama, T., Kawada, H. (2007). An Improved Shear-Lag Model for a Single Fiber Composite with a Ductile Matrix. *Key Engineering Materials*, 334-335, 333–336. doi: <https://doi.org/10.4028/www.scientific.net/kem.334-335.333>
12. Nie, J.-G., Tian, C.-Y., Cai, C. S. (2008). Effective width of steel–concrete composite beam at ultimate strength state. *Engineering Structures*, 30 (5), 1396–1407. doi: <https://doi.org/10.1016/j.engstruct.2007.07.027>
13. Timoshenko, S. P., Goodier, J. N. (1970). *Theory of Elasticity* Audio CD. New York: McGraw-Hill Book Company.
14. Suslov, V. P., Kochanov, Yu. P., Spihtarenko, V. N. (1972). *Stroitel'naya mehanika korablya i osnovy teorii uprugosti*. Leningrad: Sudostroenie, 720.
15. Eremenko, S. Yu. (1991). *Metody konechnykh elementov v mehanike deformiruemyykh tel*. Kharkiv: Izd-vo «Osnova» pri Khark. unte., 272.
16. Mozharovskiy, N. S., Kachalovskaya, N. E. (1991). *Prilozhenie metodov teorii plastichnosti i polzuchesti k resheniyu inzhenernykh zadach mashinostroeniya*. Ch. 2: *Metody i algoritmy resheniya kraevykh zadach*. Kyiv: «Vishcha shkola», 287.